Simple Modifications of the Serpin Reactive Site Loop Convert SCCA2 into a Cysteine Proteinase Inhibitor: A Critical Role for the P3′ Proline in Facilitating RSL Cleavage†

Cliff Luke,‡ Charles Schick,‡ Christopher Tsu,‡ James C. Whisstock,§ James A. Irving,§ Dieter Brömme,|| Luiz Juliano,⊥ Guo-Ping Shi,# Harold A. Chapman,# and Gary A. Silverman*,‡

Department of Pediatrics, Harvard Medical School and Division of Newborn Medicine, Children's Hospital, 300 Longwood Avenue, Boston, Massachusetts 02115, Department of Biochemistry and Molecular Biology, Monash University, Melbourne, Victoria, Australia, Department of Human Genetics, Mount Sinai School of Medicine, Fifth Avenue at 100th Street, New York, New York 10029, Department of Biophysics, Federal University of São Paulo, São Paulo, SP, Brazil 04044, and Department of Medicine, Harvard Medical School, Brigham and Women's Hospital, 75 Francis Street, Boston, Massachusetts 02115

Received January 10, 2000; Revised Manuscript Received April 3, 2000

ABSTRACT: The human squamous cell carcinoma antigens (SCCA) 1 and 2 are members of the serpin family that are 92% identical in their amino acid sequence. Despite this similarity, they inhibit distinct classes of proteinases. SCCA1 neutralizes the papain-like cysteine proteinases, cathepsins (cat) S, L, and K; and SCCA2 inhibits the chymotrypsin-like serine proteinases, catG and human mast cell chymase. SCCA2 also can inhibit catS, as well as other papain-like cysteine proteinases, albeit at a rate 50-fold less than that of SCCA1. Analysis of the mechanism of inhibition by SCCA1 revealed that the reactive site loop (RSL) is important for cysteine proteinase inhibition. The inhibition of catS by a mutant SCCA2 containing the RSL of SCCA1 is comparable to that of wild-type SCCA1. This finding suggested that there were no motifs outside and only eight residues within the RSL that were directing catS-specific inhibition. The purpose of this study was to determine which of these residues might account for the marked difference in the ability of SCCA1 and SCCA2 to inhibit papain-like cysteine proteinases. SCCA2 molecules containing different RSL mutations showed that no single amino acid substitution could convert SCCA2 into a more potent cysteine proteinase inhibitor. Rather, different combinations of mutations led to incremental increases in catS inhibitory activity with residues in four positions (P1, P3′, P4′, and P11′) accounting for 80% of the difference in activity between SCCA1 and SCCA2. Interestingly, the RSL cleavage site differed between wild-type SCCA2 and this mutant. Moreover, these data established the importance of a Pro residue in the P3′ position for efficient inhibition of catS by both wild-type SCCA1 and mutated SCCA2. Molecular modeling studies suggested that this residue might facilitate positioning of the RSL within the active site of the cysteine proteinase.

The high molecular weight serine proteinase inhibitors (serpins)[1] are a structurally well-conserved superfamily of proteins present in plants, animals, and viruses (*1*). Serpins regulate proteolytic events, associated with coagulation, fibrinolysis, apoptosis, and inflammation (reviewed in ref *2*). Previously, we cloned and characterized two human serpins, the squamous cell carcinoma antigens (SCCA) 1 and 2 (*3*−*5*). Paradoxically, SCCA1 is a potent inhibitor of the cysteine proteinases cathepsins (cat) S, L, and K (*4*), and SCCA2 (92% amino acid identity with SCCA1) is an inhibitor of the chymotrypsin-like serine proteinases catG and human mast cell chymase (*5*).

Serpins inhibit serine proteinases via a suicide substrate-like mechanism (*6*−*8*). The target proteinase binds the exposed reactive site loop (RSL) as a substrate, and the active site initiates peptide bond hydrolysis. RSL cleavage relieves strain on the metastable serpin, which then undergoes a major conformational rearrangement characterized by complete insertion of the loop into β-sheet A (*8*). Recent studies using dansyl probes to measure the proximity of the serpin and the proteinase suggest that the proteinase, covalently attached

† This work was supported from grants from the National Institutes of Health (HD28475, CA69331, and CA73031) and the Smokeless Tobacco Research Council. J.C.W. is a National Health and Medical Research Council Peter Doherty Fellow.

* To whom correspondence should be addressed at Division of Newborn Medicine, Children's Hospital, 300 Longwood Avenue, Enders 970, Boston, MA 02115-5737. Telephone: 617-355-6416. Fax: 617-355-7677. E-mail: silverman_g@a1.tch.harvard.edu.

‡ Children's Hospital.

§ Monash University.

|| Mount Sinai School of Medicine.

⊥ Federal University of São Paulo.

Brigham and Women's Hospital.

[1] Abbreviations: serpin, high molecular weight serine proteinase inhibitor; RSL, reactive site loop; PAGE, polyacrylamide gel electrophoresis; SCCA, squamous cell carcinoma antigen; cat, cathepsin; GST, glutathione S-transferase; SCCA1(2), SCCA1 with SCCA2 RSL; SCCA2(1), SCCA2 with SCCA1 RSL; SI, stoichiometry of inhibition; succ-AAPF-*p*NA, succinyl-Ala-Ala-Pro-Phe-*p*-nitroanilide; $(Z\text{-}FR)_2$-R110, $(benzyloxycarboxy\text{-}Phe\text{-}Arg)_2$-R110; RFU, relative fluorescence units; Abz, *o*-aminobenzoic acid; EDDnp, *N*-(2,4-dinitrophenyl)-ethylenediamine; MALDI, matrix-associated laser desorption ionization; MS, mass spectroscopy.

10.1021/bi000050g CCC: $19.00
Published on Web 05/20/2000

to the RSL, is translocated 70 Å towards the opposite pole of the serpin molecule (*9*). This conformational change distorts the active site of the proteinase (*10*) and traps the serpin and the enzyme in a stable covalent complex (*11*).

The RSLs of serpins play a critical role in their inhibition of serine proteinases (*8*, *12*). Analysis of the mechanism of catS inhibition by SCCA1 reveals that the RSL is utilized to inhibit cysteine proteinases as well (*13*). This notion was underscored by studies showing that the inhibitory profiles of SCCA1 and SCCA2 could be interchanged solely by swapping their RSLs. Moreover, these data suggested that there were no motifs outside and only eight residues within the RSL that confer specificity for cysteine proteinase inhibition. The purpose of this study was to take advantage of these small differences in the RSLs and to determine which residues were responsible for conferring cross-class inhibition of a cysteine proteinase.

Via site-directed mutagenesis of the RSLs of SCCA1 and SCCA2 and kinetic analysis of these mutant molecules, we determined that no single residue conferred cysteine proteinase inhibitory activity. However, when the SCCA2 RSL was altered to become more SCCA1-like, changes in four positions (P1, P3′, P4′, and P11′) accounted for 80% of the difference in catS inhibitory activity between SCCA1 and SCCA2. Moreover, the presence of a Pro residue in the P3′ position was required for efficient inhibition of catS by both wild-type SCCA1 and mutated SCCA2. Molecular modeling studies suggested that this residue facilitated inhibition by positioning the RSL into the active site of the cysteine proteinase.

EXPERIMENTAL PROCEDURES

Construction of Mutants. Mutations were generated using the QuikChange mutagenesis kit from Stratagene (La Jolla, CA) and verified by DNA sequencing, as described (*13*). Plasmid templates were pGEX/SCCA1 and pGEX/SCCA2, GST fusion protein vectors with the complete coding sequences of SCCA1 and SCCA2, respectively (*5*).

Enzymes, Inhibitors, and Substrates. SCCA mutants were purified by the bulk method using the GST fusion protein purification kit (Pharmacia, Uppsala, Sweden), as described previously (*5*). CatG and catL were purchased from Athens Research Biotech (Athens, GA). Recombinant catS and catK were prepared as described (*14*, *15*). Papain was purchased from Roche Diagnostics Corporation (Indianapolis, IN). The substrate for catG, succinyl-Ala-Ala-Pro-Phe-*p*-nitroanilide (succ-AAPF-*p*NA), was purchased from Sigma (St. Louis, MO). The catS, catK, catL, and papain substrate, (Z-Phe-Arg)$_2$-R110 [(Z-FR)$_2$-R110], was purchased from Molecular Probes (Eugene, OR). PBS reaction buffer (0.01 M phosphate buffer, 27 mM KCl, 137 mM NaCl, pH 7.4) was used with catG. Cathepsin reaction buffer, pH 5.5 (50 mM sodium acetate, pH 5.5, 4 mM dithiothreitol, and 1 mM EDTA), was used with catS.

Elastin Degradation. Bovine neck ligament elastin was labeled as described (*16*). The catS elastinolytic activity was determined as described (*17*). Fractional activity was the amount of ^{3}H released into the supernatant by catS in the presence (average cpm$_i$)/absence (average cpm$_ø$) of inhibitor. The means of the counts were obtained from quadruplicate samples (the standard deviation of the samples was less than 15% of the mean).

Kinetics. As an initial test for inhibitor activity, proteinase and molar excess (~2−100 fold) of SCCA or SCCA mutant were incubated for 30 min at 25 °C, in the appropriate reaction buffer, as described (*5*). Residual enzyme activity was measured by the addition of substrate. Activity of enzyme in the presence of inhibitor was compared to an uninhibited control. The inhibition of catS and papain by SCCA and the mutants was measured under pseudo-first-order conditions using the progress curve method (*18*), as described (*5*), and fit via nonlinear regression to

$$P = (v_z/k_{obs}) \times [1 - e^{(-k_{obs}t)}] \quad (1)$$

In this model, the progress of enzyme activity, as expressed by product formation (P), begins at a rate (v_z) and slows (due to inhibition) over time at a first-order rate (k_{obs}). The rate constant is dependent only on inhibitor concentration. A second-order rate constant, k', was determined by plotting the k_{obs} versus the respective inhibitor concentration [I] and measuring the slope of the line ($k' = \Delta k_{obs}/\Delta[I]$). The second-order rate constant (k') was corrected (k_{ass}) to take into account the substrate concentration [S] and the K_m of the enzyme for the substrate as represented by

$$k_{ass} = (1 + [S]/K_m) \times k' \quad (2)$$

For each inhibitor, the first-order rates of inhibition were measured at different inhibitor concentrations (at least four). Calculation of the second-order rate constant required a linear relationship between the first-order rate constant and the inhibitor concentration.

The rate of association of inhibitor with catG was determined under second-order conditions (*19*), as described (*5*), using

$$1/[E]_f = 1/[E]_o + k_{ass}t \quad (3)$$

In this model, the reciprocal of the concentration of free enzyme ($1/[E]_f$) over time (t) has a slope of the second-order rate constant (k_{ass}) with an intercept of the reciprocal of the concentration of total (bound and free) enzyme ($1/[E]_o$). Second-order rate constants were determined at several different equimolar enzyme and inhibitor concentrations. The calculation of the second-order rate constant required a linear relationship between the reciprocal of free enzyme ($1/[E]_o$) and time (s) over at least five time points and an intercept equivalent to the reciprocal of the total enzyme concentration. All kinetic data were fit using GraphPad Prism 2.0a for Power Macintosh (GraphPad Software Inc, San Diego, CA).

Stoichiometry of Inhibition (SI). The SI for SCCA1, SCCA2, and several of the mutants were determined under conditions as described (*4*).

Thermostability Assays. Aliquots of recombinant serpin proteins were incubated for 5 min at temperatures ranging from 55 to 100 °C. Samples were centrifuged, and the supernatant was removed. Protein content was assessed by a Bradford-based protein assay kit and SDS−PAGE.

Peptides. Peptides were synthesized as described (*20*, *21*). For kinetic analysis, 3−30 μM uncleaved peptide was incubated with 20−30 nM catS in 100 μL of cathepsin reaction buffer, pH 5.5. The rate of substrate cleavage (RFU/min) was measured at different enzyme and substrate concentrations, using a fMax fluorescent plate reader (Ex =

Table 1: SCCA2 RSL Mutants

	serpin	RSL[a]: proximal hinge P	14	13	12	11	10	9	variable 8	7	6	5	4	3	2	1	1′	2′	3′	4′	5′	6′	distal hinge 11′	k_{ass} (10^3 M^{-1} s^{-1})[b] catS	catG
A	SCCA1[c]		G	*A*	E	A	A	A	A	T	A	V	V	*G*	*F*	*G*	*S*	S	*P*	*T*	S	T	H	100	0
B	SCCA2[d]		G	**V**	E	A	A	A	A	T	A	V	V	**V**	**V**	**E**	**L**	S	**S**	**P**	S	T	**C**	2.4	118
C	SCCA1(2)[e,f]		.	**V**	.	.	.	.	.	.	.	.	.	**V**	**V**	**E**	**L**	.	**S**	**P**	.	.	**C**	1.4	65
D	V341R		.	R	.	.	.	.	.	.	.	.	.	.	.	.	.	.	.	.	.	.	.	0	0
E	V351G		.	.	.	.	.	.	.	.	.	.	.	*G*	.	.	.	.	.	.	.	.	.	2.8	108
F	V352F		.	.	.	.	.	.	.	.	.	.	.	.	*F*	.	.	.	.	.	.	.	.	2.2	5
G	V341R, V352F		.	R	.	.	.	.	.	.	.	.	.	.	*F*	.	.	.	.	.	.	.	.	0	0
H	E353G		.	.	.	.	.	.	.	.	.	.	.	.	.	*G*	.	.	.	.	.	.	.	15	57
I	L354S		.	.	.	.	.	.	.	.	.	.	.	.	.	.	*S*	.	.	.	.	.	.	4.0	0
J	V341T		.	T	.	.	.	.	.	.	.	.	.	.	.	.	.	.	.	.	.	.	.	4.8	120
K	C364H		.	.	.	.	.	.	.	.	.	.	.	.	.	.	.	.	.	.	.	.	*H*	4.6	32
L	S356P, P357T		.	.	.	.	.	.	.	.	.	.	.	.	.	.	.	.	*P*	*T*	.	.	.	9.1	0
M	S356P, P357T, C364H		.	.	.	.	.	.	.	.	.	.	.	.	.	.	.	.	*P*	*T*	.	.	*H*	6.8	0
N	V351G, V352F		.	.	.	.	.	.	.	.	.	.	.	*G*	*F*	.	.	.	.	.	.	.	.	3.9	7
O	V341R; V351G, V352F		.	R	.	.	.	.	.	.	.	.	.	*G*	*F*	.	.	.	.	.	.	.	.	0	0
P	V351G, V352F, S356P, P357T		.	.	.	.	.	.	.	.	.	.	.	*G*	*F*	.	.	.	*P*	*T*	.	.	.	10	0
Q	V341T, V351G, V352F, S356P, P357T		.	T	.	.	.	.	.	.	.	.	.	*G*	*F*	.	.	.	*P*	*T*	.	.	.	9.9	0
R	V351G, V352F, E353G, S356P, P357T		.	.	.	.	.	.	.	.	.	.	.	*G*	*F*	*G*	.	.	*P*	*T*	.	.	.	60	0
S	V351G, V352F, E353G, L354S, S356P, P357T		.	.	.	.	.	.	.	.	.	.	.	*G*	*F*	*G*	*S*	.	*P*	*T*	.	.	.	59	0
T	E353G, S356P, P357T		.	.	.	.	.	.	.	.	.	.	.	.	.	*G*	.	.	*P*	*T*	.	.	.	43	0
U	E353G, S356P, P357T, C364H		.	.	.	.	.	.	.	.	.	.	.	.	.	*G*	.	.	*P*	*T*	.	.	*H*	78	0
V	SCCA2(1)[f,g]		.	*A*	.	.	.	.	.	.	.	.	.	*G*	*F*	*G*	*S*	.	*P*	*T*	.	.	*H*	120	0

[a] Schechter and Berger numbering scheme (*26*). P1 = residue 353. Plain type residues are common to both SCCA1 and SCCA2, bold residues are SCCA2-specific, italicized residues are SCCA1-specific, underlined residues are novel to both SCCA1 and SCCA2, and black dots refer to SCCA2 sequences. [b] catS = cathepsin S; catG = cathepsin G. Second-order rate constants were calculated under second-order conditions (catG) and pseudo-first-order conditions (catS). 0 = no inhibition seen under conditions used. [c] Ref *4*. The functional P1 residue for the SCCA1−catS interaction is the G353 residue. [d] Ref *5*. The functional P1 residue for the SCCA2−catG interaction is the L354 residue. [e] SCCA1 framework with SCCA2 RSL. [f] Ref *13*. [g] SCCA2 framework with SCCA1 RSL.

345 nm, Em = 445 nm). The concentration of cleaved peptide per RFU (M/RFU) was calculated using a standard curve of completely digested peptide (peptide 1). The weak affinity of catS for these peptides precluded the separate determination of K_m and k_{cat}. Under these conditions, the combined second-order substrate specificity constant [k_{cat}/K_m (M^{-1} s^{-1})] can be determined by

$$v_i = (k_{cat}/K_m)[E]_0[S]_I \quad (4)$$

where v_i is the calculated velocity (M/s), $[E]_0$ is the total enzyme concentration, and $[S]_I$ is the substrate concentration (M). The linear slope of velocity versus substrate concentration, divided by the total enzyme concentration, is the k_{cat}/K_m.

Modeling. The model of SCCA1 was built using MODELLER (*22*) and Quanta98 (M.S.I. Inc, San Diego) using the X-ray crystal structure of native α1-antitrypsin (PDB identifier 2psi) as a template. The coordinates of catL and K (*23*, *24*) were obtained from the Protein Data Bank (PDB identifiers 1cjl and 1ayu, respectively). The coordinates of catS have not been deposited, but a theoretical model (PDB identifier 1bxf) built by Fengler et al. (*25*) was used to construct a catS−SCCA1 complex. The structure of cruzain in complex with the inhibitor benzoyl-tyrosine-alanine-fluoromethyl ketone (PDB identifier 1aim) and actinidin in complex with the inhibitor E64 (PDB identifier 1aec) were used as templates to homology model the P3−P1 residues of SCCA1 into the active site of catL. The complexes between SCCA1 and catL, K, and S were built using the modeling tools available in Quanta98 and subjected to CHARMm minimization. The dihedral angles of each model were checked, and those residues that were outside allowed regions were subjected to dihedral constraints and further rounds of CHARMm minimization until all residues were in allowed conformations.

Analysis of Cleavage of the RSL by Matrix-Associated Laser Desorption Ionization (MALDI) MS. The serpin (10 μM) and either catS (2 μM) or papain (1 μM) were prepared (*13*), and the components were separated by MALDI MS at the Wistar Protein Microchemistry Facility (Philadelphia).

RESULTS

Inhibition of catS by Wild-Type SCCA2. Typically, residues in serpin RSLs are identified using the Schechter−Berger numbering scheme (*26*). However, relative to the P1 Met358 for the archetypal serpin α1-antitrypsin (α1-antiproteinase inhibitor) (*27*) and the Leu354 of SCCA2 (*5*), the functional P1 residue (Gly353) for the SCCA1−catS interaction is located at the canonical P2 position (*13*). Thus, in keeping with the numbering scheme for peptide substrates, the RSLs of SCCA1 and SCCA2 were renumbered relative to the actual P1 of SCCA1 (Table 1, serpins A and B).

Since the RSL of SCCA1 can function in the framework of SCCA2 (Table 1, serpin V and ref *13*) and the RSLs of SCCA1 and SCCA2 differ by only eight residues (Table 1, serpins A and B), we hypothesized that these amino acids were important determinants of cysteine proteinase inhibition. To test this hypothesis, we employed a strategy of mutating the RSLs of both SCCA2 and SCCA1 and assessing their gain and loss of catS inhibitory activity, respectively. Note,

Table 2: SCCA1 RSL Mutants

		RSL[a]: proximal hinge							variable													distal hinge	k_{ass} (10^3 M^{-1} s^{-1})[b]	
	serpin	P	14	13	12	11	10	9	8	7	6	5	4	3	2	1	1′	2′	3′	4′	5′	6′	11′	catS	catG
A	SCCA1[c]		G	*A*	E	A	A	A	A	T	A	V	V	*G*	*F*	*G*	*S*	S	*P*	*T*	S	T	H	100	0
B	SCCA2[d]		G	**V**	E	A	A	A	A	T	A	V	V	**V**	**V**	**E**	**L**	S	**S**	**P**	S	T	**C**	2.4	118
C	SCCA1(2)[e,f]		.	**V**	.	.	.	.	.	.	.	.	.	**V**	**V**	**E**	**L**	.	**S**	**P**	.	.	C	1.4	65
D	F352A[f]		.	.	.	.	.	.	.	.	.	.	.	.	A	.	.	.	.	.	.	.	.	0	0
E	G353E[f]		.	.	.	.	.	.	.	.	.	.	.	.	.	**E**	.	.	.	.	.	.	.	110	
F	A341T[f]		.	T	.	.	.	.	.	.	.	.	.	.	.	.	.	.	.	.	.	.	.	390	
G	H364C		.	.	.	.	.	.	.	.	.	.	.	.	.	.	.	.	.	.	.	.	**C**	82	
H	S354L		.	.	.	.	.	.	.	.	.	.	.	.	.	.	**L**	.	.	.	.	.	.	50	0
I	P356G		.	.	.	.	.	.	.	.	.	.	.	.	.	.	.	.	G	.	.	.	.	12	0

[a] Schechter and Berger numbering scheme (*26*). P1 = residue 353. Plain type residues are common to both SCCA1 and SCCA2, bold residues are SCCA2-specific, italicized residues are SCCA1-specific, underlined residues are novel to both SCCA1 and SCCA2, and black dots refer to SCCA1 sequences. [b] catS = cathepsin S; catG = cathepsin G. Second-order rate constants were calculated under second-order conditions (catG) and pseudo-first-order conditions (catS). 0 = no inhibition seen under conditions used. [c] Ref *4*. The functional P1 residue for the SCCA1−catS interaction is the G353 residue. [d] Ref *5*.The functional P1 residue for the SCCA2−catG interaction is the L354 residue. [e] SCCA1 framework with SCCA2 RSL. [f] Ref *13*.

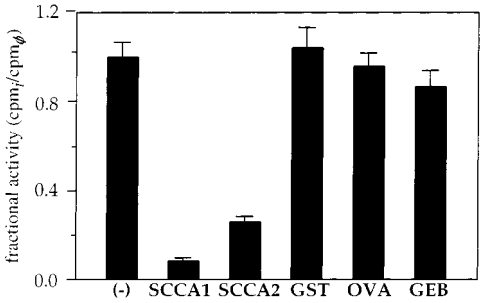

FIGURE 1: Inhibition of catS-mediated elastinolytic degradation by SCCA2. Ability of SCCA2 to inhibit the elastinolytic activity of catS was measured using an in vitro elastin degradation assay. SCCA1, SCCA2, ovalbumin (OVA), GST (20 nM each), and glutathione elution buffer (GEB) were incubated with catS (20 nM) for 16 h at 37 °C in wells coated with [^{3}H]elastin, as described (*4*). Fractional activity was the amount of ^{3}H released into the supernatant by catS in the presence (average cpm$_i$)/absence (average cpm$_\phi$) of inhibitor.

that the RSL swap mutants (Tables 1 and 2) and a few of the SCCA1 mutants (Table 2) were reported previously (*13*). They are included here to facilitate comparisons and are identified by footnotes in the tables. All kinetic analyses were performed at least three times with a variability of <10% with the exception of SCCA2 and catS in which the variability was ∼15%.

Although SCCA2 is an inhibitor of the chymotrypsin-like serine proteinases, catG, and mast cell chymase, preliminary studies suggested that SCCA2 could inhibit (albeit to a much lesser degree than SCCA1) the catalytic activity of catS. This was demonstrated in two ways. First, we measured the ability of SCCA2 to inhibit catS degradation of a complex substrate, [^{3}H]elastin. CatS was incubated with or without SCCA2 for >16 h in wells coated with [^{3}H]elastin. A reduction in the amount of [^{3}H]elastin released into the supernatant in the presence of SCCA2 (as compared to that of the no-serpin control) was an indication of catS inhibition. SCCA2 inhibited the catS-mediated degradation of elastin by ∼70%, whereas SCCA1 decreased elastolytic activity by ∼90% (Figure 1).

Second, we determined the baseline kinetics of the SCCA2−catS interaction using small fluorogenic peptide substrates and the progress curve method. At high concentrations of SCCA2, we measured a catS inhibition rate of k_{ass} = 2.4 × 10^3 M^{-1} s^{-1} (Figure 2; Table 1, serpin B). This relatively low rate of inhibition may have been an artifact of the high inhibitor concentrations used to measure the second-order rate constant. To rule out the presence of a noninhibitory interaction, we generated the SCCA2 P13 mutant [Val341Arg]. Typically, a charged residue at this

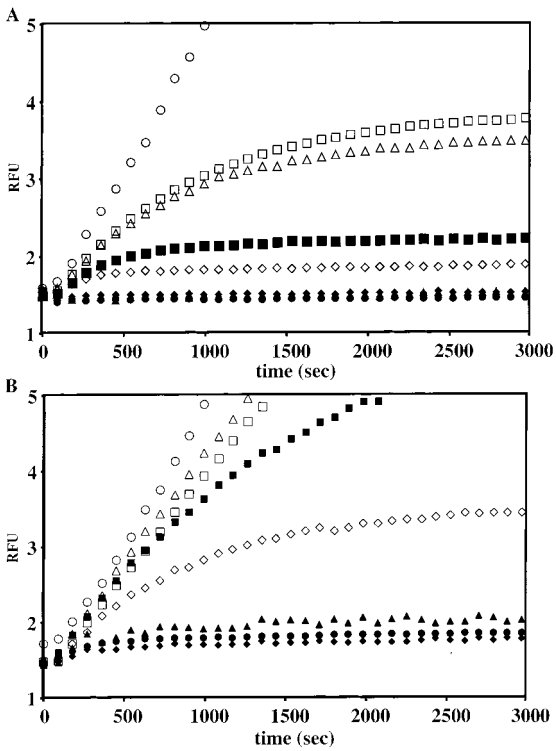

FIGURE 2: Kinetic analysis of SCCA1, SCCA2, and mutants. Effect of mutations on the inhibition of catS was measured under pseudo-first-order conditions using the progress curve method. Inhibitor concentrations were at 500 nM (A) or 150 nM (B). SCCA2 (□); SCCA2 P11′ mutant [Cys364His] (△); SCCA2 P3′, 4′ mutant [Ser356Pro, Pro357Thr] (■); SCCA2 P1 mutant [Glu353Gly] (◇); SCCA2 P1, 3′, 4′ mutant [Glu353Gly, Ser356Pro, Pro357Thr] (◆); SCCA2 P1, 3′, 4′, 11′ mutant [Glu353Gly, Ser356Pro, Pro357Thr, Cys364His] (▲); and SCCA1 (●) were incubated with catS (10 nM) and substrate ([(Z-FR)$_2$-R110] at 5 μM) at 25 °C in cathepsin buffer 5.5. CatS without inhibitor (○) served as a control. Progress of catS inactivation was followed by measuring the relative fluorescence (RFU) over time. A set of curves from a representative experiment is depicted.

position abolishes serpin inhibitory activity but does not inhibit proteinase binding or RSL cleavage (*8*, *12*, *13*, *28*). Not only was this mutant inactive against catG, but even at high concentrations, this mutant failed to inhibit catS (Table 1, serpin D). These data suggested that SCCA2 could inhibit catS but at a rate 50-fold slower than that of SCCA1.

Effects of Single Amino Acid Changes. Of the eight amino acids that could contribute to the 50-fold difference in the rates of catS inhibition by SCCA1 and SCCA2, one is located in the proximal hinge region (P13), one is located in the distal hinge region (P11′), and six flank the cleavage site (P3−P4′). Since residues in the proximal and distal hinge regions affect RSL mobility or conformation, but are less likely to contribute to target specificity as determined by active site binding, we focused initially on the four different residues that would interact most directly with the active site of the cysteine proteinase (P3−P1′).

Unlike the serine proteinases, such as trypsin and chymotrypsin, which show specificity for the amino acid N-terminal to the cleavage site (P1), papain-like cysteine proteinases, such as catS, show greater specificity for the P2 residue. In particular, catS prefers the hydrophobic residues Leu > Phe > Val at this position while being much less specific at the P1 position (*13*−*15*, *29*). Indeed, in previous work, an SCCA1 P2 mutant [Phe352Ala] lost catS inhibition (Table 2, serpin D), whereas a P1 mutant [Gly353Glu] inhibited catS at the same rate as the wild-type protein (Table 2, serpin E) (*13*). We generated several single-change mutants of SCCA2 by substituting for the corresponding SCCA1 residues. The SCCA2 P3 mutant [Val351Gly], P2 mutant [Val352Phe], and P1′ mutant [Leu354Ser] showed only a marginal effect on catS inhibitory activity relative to that of wild-type SCCA2 (Table 1, serpins E, F, I, and B, respectively). These data showed that the presence of the favored Phe residue at the P2 position was in itself insufficient to augment catS inhibition. However, we should not infer that the residues at these other positions are irrelevant to catS inhibition. An SCCA1 P1′ mutant [Ser354Leu], which harbors an SCCA2 residue at the P1′, showed a 50% decrease in the rate of catS inhibition ($k_{ass} = 50 \times 10^3$ M^{-1} s^{-1}) relative to that of wild-type SCCA1 (Table 2, serpin H and A, respectively).

In contrast to the P3, P2, and P1′ mutants, the SCCA2 P1 mutant [Glu353Gly] showed a 6-fold increase in the rate of catS inhibition ($k_{ass} = 15 \times 10^3$ M^{-1} s^{-1}) relative to that of wild-type SCCA2 (Table 1, serpins H and B, respectively). These findings were somewhat surprising considering that a Phe at the P2 residue was essential for catS inhibition (Table 2, serpin D) and Glu at the P1 position was well tolerated in the SCCA1 mutants described above (Table 2, serpin E) (*13*).

Next, we focused on single mutations in the hinge regions. SCCA2, unlike other ov-serpins, contains a Val rather than a typical Thr at the P13 proximal hinge region position (the canonical P14 residue in α1-antitrypsin). Although SCCA1 contains an Ala rather than the consensus Thr at this position, an SCCA1 P13 mutant [Ala342Thr] showed nearly a 4-fold increase in the rate constant for the SCCA1−catS interaction (Table 2, mutant F) (*13*). However, an SCCA2 P13 mutant [Val342Thr] showed only a 2-fold increase in its rate of interaction with catS ($k_{ass} = 4.8 \times 10^3$ M^{-1} s^{-1}) (Table 1, serpin J). Similarly, mutation of the P11′ distal hinge position of SCCA2 to that of SCCA1 yielded an SCCA2 P11′ mutant [Cys364His] that showed only a 2-fold increase its rate of catS inhibition ($k_{ass} = 4.6 \times 10^3$ M^{-1} s^{-1}) (Table 1, serpin K). Interestingly, the converse SCCA1 P11′ mutant [His364Cys] showed a ∼20% decrease in the rate constant ($k_{ass} = 82 \times 10^3$ M^{-1} s^{-1}) (Table 2, serpin G). This finding suggested that differences between SCCA1 and SCCA2 at the P11′ position, as well as at the P1′ position noted above, were not due to random substitutions and that these residues contributed to the inhibition of catS. Collectively, however, these data also showed that no single residue in the RSL of SCCA2 could be altered such that the mutant molecule could inhibit catS at a rate comparable to that of SCCA1.

Effects of the P3′ Proline. Crystallographic data suggest that the subsite residues of papain-like cysteine proteinases extend two to three residues beyond (C-terminal to) the substrate cleavage site (*29*). These findings suggest that downstream P′ residues of the RSL will affect inhibitory activity. A subtle difference between SCCA1 and SCCA2 is the position of the downstream Pro residue. In SCCA1, a Pro residue is located in the P3′ position, whereas in SCCA2 it is located in the P4′ position. Proline is an important structural residue and may play a role in the overall conformation and flexibility of the RSL. The importance of this P3′ residue for catS inhibition was demonstrated by the SCCA1 P3′ mutant [Pro356Gly]. Substitution of the more mobile Gly residue caused a 90% reduction in the rate of catS inhibition ($k_{ass} = 12 \times 10^3$ M^{-1} s^{-1}) relative to that of wild-type SCCA1 (Table 2, serpin I and A, respectively). To determine whether shifting the ProP4′ in SCCA2 to the P3′ position would have an effect on catS inhibitory activity, we generated the SCCA2 P3′, P4′ mutant [Ser356Pro, Pro357Thr]. A double mutant was used to avoid creating a ProP3′−ProP4′ and to recapitulate the ProP3′−ThrP4′ motif observed in SCCA1. This double mutant demonstrated almost a 5-fold increase in the rate of catS inhibition ($k_{ass} = 9.0 \times 10^3$ M^{-1} s^{-1}) relative to that of wild-type SCCA2 (Table 1, serpin L and B, respectively). These results suggested that the ProP3′ is an important determinant of catS inhibition by these serpins.

Effects of Multiple Amino Acid Changes. The results suggested that when either the P1 or P3′−P4′ residues of SCCA2 were mutated to those of SCCA1, the rate of catS inhibition increased 5−6-fold. To determine whether the effects of these and the other mutations were synergistic, we constructed a series of mutant molecules by combining several of the changes noted above. Initially, we focused on the critical P2 residue. Conceivably, the lack of inhibitory activity associated with the SCCA2 P2 mutant [Val352Phe] was due to its incompatibility with the flanking P3 or P1 residue (Table 1, serpin F). Since an SCCA1 mutant [Gly353Glu] (wild-type residue for SCCA2) showed enhanced activity against catS (Table 2, serpin E), we concluded that the PheP2−GluP1 motif should not in itself interfere with the activity of the SCCA2 P2 mutant [Val352Phe]. Thus, we generated a double mutant in which only the P3 and P2 residues were converted to those present in SCCA1. However, this SCCA2 P3, P2 double mutant [Val351Gly, Val352Phe] showed only a marginal increase in catS inhibitory activity (2.2 vs 3.9 × 10^3 M^{-1} s^{-1}) (Table 1, serpin N). Nonetheless, this small increment in inhibitory activity was specific for the RSL, as an SCCA2 P13, P3, P2

mutant [Val341Arg, Val351Gly, Val352Phe] lost completely inhibitory activity (Table 1, serpin O).

To determine whether an incremental increase in inhibitory activity could be observed with additional mutations, we next generated an SCCA2 P3, P2, P3′, P4′ mutant [Val351Gly, Val352Phe, Ser356Pro, Pro357Thr]. Despite the presence of these four mutations, the inhibitory activity of this molecule was no different than that of the SCCA2 P3′, P4′ mutant [Ser356Pro, Pro357Thr] ($k_{ass} = \sim 10 \times 10^3$ M^{-1} s^{-1}) (Table 1, serpin P and L, respectively). Even a substitution for the favorable Thr residue at the P13 position, which yielded the SCCA2 P13, P3, P2, P3′, P4′ mutant [Val341Thr, Val351Gly, Val352Phe, Ser356Pro, Pro357Thr], did not increase inhibitory activity ($k_{ass} = 9.9 \times 10^3$ M^{-1} s^{-1}) (Table 1, serpin Q). However, a substitution for the GlyP1 to generate an SCCA2 P3, P2, P1, P3′, P4′ mutant [Val351Gly, Val352Phe, Glu353Gly, Ser356Pro, Pro357Thr] showed a more pronounced increase in inhibitory activity ($k_{ass} = 60 \times 10^3$ M^{-1} s^{-1}) (Table 1, serpin R). This increase in activity was 6-fold greater than the SCCA2 P3′, P4′ mutant [Ser356Pro, Pro357Thr] (Table 1, serpin L) and 25-fold greater than that of wild-type SCCA2 (Table 1, serpin B). Addition of the final binding site mutation at the P1′ site generated an SCCA2 P3, P2, P1, P1′, P3′, P4′ mutant [Val351Gly, Val352Phe, Glu353Gly, Leu354Ser, Ser356Pro, Pro357Thr] that did not show a further increase in catS inhibitory activity ($k_{ass} = 59 \times 10^3$ M^{-1} s^{-1}) (Table 1, serpin S).

The increased catS inhibitory activity associated with the SCCA2 P3, P2, P1, P3′, P4′ mutant [Val351Gly, Val352Phe, Glu353Gly, Ser356Pro, Pro357Thr] (Table 1, serpin R) was unanticipated since substituting the GlyP1 should have shown no improvement over a GluP1 [the SCCA1 P1 mutant [Gly353Glu] showed no enhancement of catS inhibitory activity (Table 2, serpin E)]. Thus, the increased activity associated with the [Glu353Gly] mutation at the P1 position may have been due to its association with the ProP3′−ThrP4′ residues and was independent of the GlyP3−PheP2 motif. This association appeared to be the case as the more simpler SCCA2 P1, P3′, P4′ mutant [Glu353Gly, Ser356Pro, Pro357Thr] (Table 1, serpin T) demonstrated 4-fold greater catS inhibitory activity relative to that of the SCCA2 P3′, P4′ mutant [Ser356Pro, Pro357Thr] (Table 1, serpin L) and 18-fold greater inhibitory activity than that of wild-type SCCA2 (Table 1, serpin B). Finally, when a substitution at the P11′ position was used to generate an SCCA2 P1, P3′, P4′, P11′ mutant [Glu353Gly, Ser356Pro, Pro357Thr, Cys364His], the rate of catS inhibition increased a further 2-fold ($k_{ass} = 78 \times 10^3$ M^{-1} s^{-1}) (Table 1, serpin U) over the SCCA2 P1, P3′, P4′ mutant [Glu353Gly, Ser356Pro, Pro357Thr] (Table 1, serpin T) and 32-fold over that of wild-type SCCA2 (Table 1, serpin B). Thus, by substituting SCCA2 residues for those of SCCA1 at the P1, P3′, P4′, and P11′ positions, SCCA2 achieved a rate of catS inhibition that was ~80% that of SCCA1.

Effects of Mutations on RSL Stability and Stoichiometry of Inhibition. Conceivably, mutations in the RSLs could affect stability of the serpin molecules. For example, a mutation could facilitate insertion of the RSL into the β-sheet A, thereby forming inactive molecules in the latent conformation. Unlike wild-type, metastable serpins in the active conformation, loop-inserted variants are more stable and do not precipitate when incubated at temperatures from 65 to 90 °C. Since most of the serpins were active for either catS or catG (except the P13 mutants, Table 1), it is unlikely that the mutants reverted to the latent conformation. Thermostability curves for SCCA1, SCCA2, SCCA2 mutants ([Glu353Gly], [Ser356Pro, Pro357Thr], [Glu353Gly, Ser356Pro, Pro357Thr, Cys364His]) and SCCA2(1) confirmed this notion as all of these serpins were precipitated completely by heating to 85 °C (data not shown).

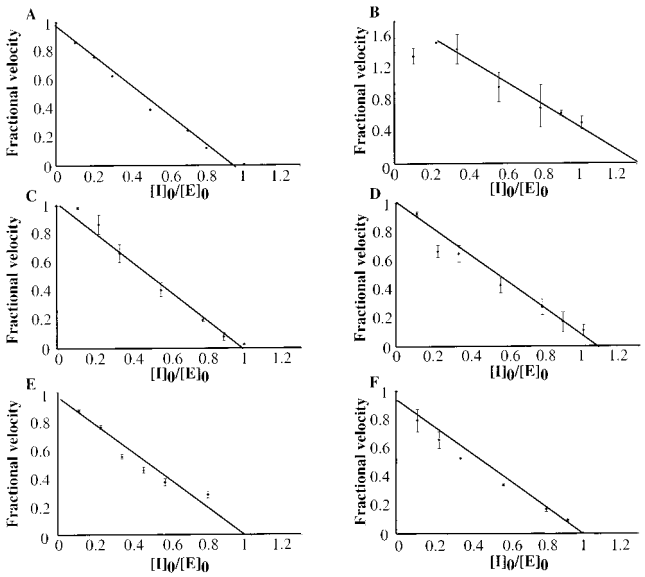

FIGURE 3: Stoichiometry of inhibition. (A) catS (35 nM) and SCCA1 (0−36 nM), (B) catS (3.4 μM) and SCCA2 (0−3.4 μM), (C) catS (177 nM) and SCCA2 mutant [E353G] (0−177 nM), (D) catS (177 nm) and SCCA2 mutant [S356P, P357T] (0−177 nM), (E) catS (35 nM) and SCCA2 mutant [E353G, S356P, P357T, C364H] (0−40 nM), (F) catS (35 nM) and SCCA2(1) (0−40 nM) were incubated for 30 min at 25 °C in cathepsin reaction buffer. Fractional velocity was calculated by the addition of substrate [$(Z\text{-}FR)_2$-R110] and by measuring the ratio of the velocity of inhibited enzyme (v_i) to the velocity of the uninhibited control (v_0). Stoichiometry of inhibition (SI) was determined by plotting the fractional velocity against different inhibitor [I_0]/enzyme [E_0] ratios and using linear regression analysis to extrapolate to that [I_0]/[E_0] ratio resulting in complete inhibition.

The mutations within the RSL of SCCA2 might also lead to an apparent rate reduction with catS due to a relative increase in flux along the substrate branch of the inhibitory pathway. One means to assess this possibility is to determine the stoichiometry of the catS inhibitory reaction. Typically, serpins bind and inhibit their target proteases at 1:1 stoichiometry (SI = 1). However, if a parallel substrate reaction occurs, the SI > 1. Because of the limits of our assay system, only mutants with an appreciable increase on the k_{ass} were selected for analysis. For SCCA1 (control), the SCCA2 mutants ([Glu353Gly], [Ser356Pro, Pro357Thr], [Glu353Gly, Ser356Pro, Pro357Thr, Cys364His]) and SCCA2(1), the SIs $\approx$ 1 (Figure 3). The SI for the SCCA2−catS interaction also was $\approx$1. However, the high concentrations of inhibitor and enzyme required to perform the analysis and the relatively low k_{ass} increased the variability of this measurement (Figure 3B).

Peptide Analysis. Of all of the mutations analyzed, the presence of a Pro residue at the P3′ position appeared to be important for catS inhibition. The ProP3′ lies at the edge of the peptide binding groove of catS and may have important implications in designing active site inhibitors for papain-

Table 3: CatS Interaction with Self-Quenching Fluorescent Peptides

peptide	name (modeled RSL)	peptide(P4−P5′)[a] 4	3	2	1	1′	2′	3′	4′	5′	k_{cat}/K_m ($\times 10^4$ M^{-1} s^{-1})
1	SCCA1	V	*G*	*F*	*G*	*S*	S	*P*	*T*	S	2.3
2	SCCA1 P356G	V	*G*	*F*	*G*	*S*	S	G	*T*	S	0.9
3	SCCA1 P356S, T357P	V	*G*	*F*	*G*	*S*	S	**S**	**P**	S	0.7

[a] In the form of Abz-peptide-Gln-EDDnp. Plain type residues are common to both SCCA1 and SCCA2, italicized residues are SCCA1-specific, bold residues are SCCA2-specific, and underlined residues are novel to both SCCA1 and SCCA2.

like cysteine proteinases. To further analyze the effect of the ProP3′ on the binding and the catalysis of the RSL, we simplified our analysis by using self-quenching fluorescent peptides modeled after the SCCA1 RSL sequence from P4−P5′. (*20*, *21*, *30*). This approach allowed for an analysis of the early steps of RSL binding and cleavage independent of the gross conformational changes associated with serpin inhibitory function. In addition, it is often possible to determine the k_{cat} and K_m of the interaction. These values could provide insight into which peptide residues contribute to the binding (K_m) or catalysis (k_{cat}) of the interaction with catS. Unfortunately, measurement of the K_m of the interaction with catS required the use of high concentrations of peptide substrate, which resulted in considerable intermolecular quenching of the cleaved substrate. Thus, only the combined pseudo-second-order rate constant k_{cat}/K_m could be calculated reliably.

Changes in the k_{cat}/K_m rates determined in the peptides correlated well with those changes observed with the intact serpin (Table 3). The peptide with the wild-type SCCA1 RSL sequence (Table 3, peptide 1) had a k_{cat}/K_m of 2.3×10^4 M^{-1} s^{-1}. Peptides containing [ProP3′Gly] (Table 3, peptide 2) and [ProP3′Ser, ThrP4′Pro] (Table 3, peptide 3) mutations demonstrated a k_{cat}/K_m that was 60% (9.0×10^{-3} M^{-1} s^{-1}) and 70% (7.4×10^{-3} M^{-1} s^{-1}) slower than that of peptide 1 (SCCA1 RSL), respectively. These results suggested that Pro at the P3′ position of SCCA1 was involved in catS inhibition by increasing the binding and/or cleavage of the substrate-like RSL.

SCCA2 Activity against Other Papain-Like Cysteine Proteinases. To determine whether SCCA2 and some of the other mutants harbored inhibitory activity against other cysteine proteinases, we incubated these serpins with either catK, catL, or papain (I:E = 20:1). The percent inhibitions showed the same relative trend as that for catS inhibition [i.e., the closer the mutations in the RSL of SCCA2 to SCCA1, the greater the percent inhibition (data not shown)]. To examine this trend kinetically, the interactions between SCCA2 and the SCCA2 mutant [Glu353Gly, Ser356Pro, Pro357Thr, Cys364His] with papain were assessed (Figure 4). The SI and the k_{ass} of the SCCA2−papain interaction were 1.6 and 3×10^3 M^{-1} s^{-1}, respectively. For the SCCA2 mutant [Glu353Gly, Ser356Pro, Pro357Thr, Cys364His]−papain interaction, the values were 1.4 and 1.65×10^5 M^{-1} s^{-1} (Figure 4). Thus, like SCCA1 (*4*), SCCA2 and several of the mutants could inhibit other types of papain-like cysteine proteinases.

Cleavage of the SCCA2 RSL by catS and Papain. To determine where the cysteine proteinases cleave the RSL, SCCA2 was mixed with either catS (I:E = 5:1) or papain (I:E = 10:1), and the cleavage products were analyzed by MALDI MS. If catS and papain cleaved SCCA2 within the

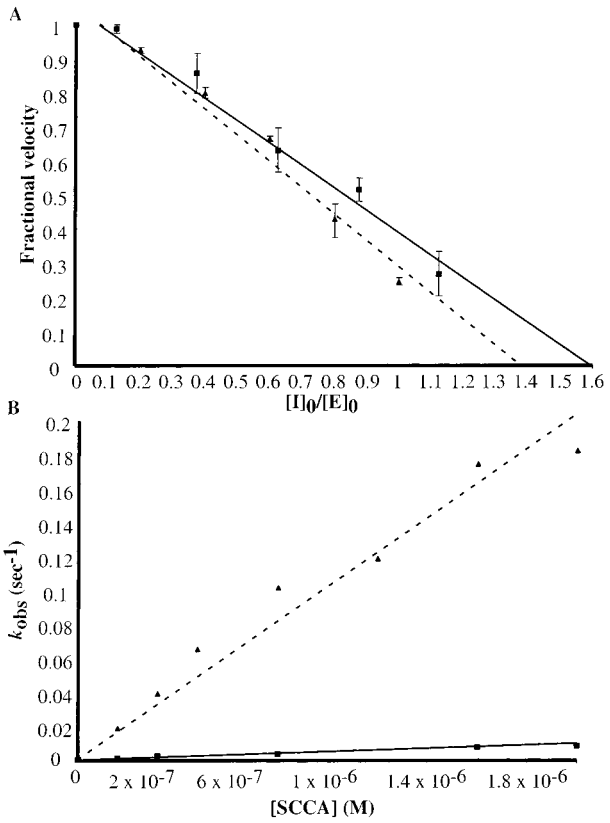

FIGURE 4: SCCA2−papain interactions. (A) Stoichiometry of inhibition for SCCA2 (0−160 nM) (■) and SCCA2 mutant [E353G, S356P, P357T, C364H] (0−160 nM) (▲) with papain (160 nM). Enzyme and inhibitor were incubated for 30 min at 25 °C in cathepsin reaction buffer. Fractional velocity was calculated by the addition of substrate [(Z-FR)$_2$-R110] and by measuring the ratio of the velocity of inhibited enzyme (v_i) to the velocity of the uninhibited control (v_0). Stoichiometry of inhibition (SI) was determined by plotting the fractional velocity against different inhibitor [I_0]/enzyme [E_0] ratios and using linear regression analysis to extrapolate to that [I_0]/[E_0] ratio resulting in complete inhibition. This gave an SI for SCCA2 of 1.6 (solid line) and for the mutant, 1.4 (dashed line). (B) Rate of inhibition for SCCA2 (0−8 μM) and the SCCA2 mutant [E353G, S356P, P357T, C364H] (0−2 μM) against papain 160 nM). Papain was added to either SCCA2 (■) or the mutant (▲) plus the subtrate [(Z-FR)$_2$-R110, 10 μM], and the RFU was measured over time. Curves were then subjected to nonlinear regression analysis using eq 1. The rate (k_{obs}) was then plotted against the serpin concentration, and the lines were fitted using eq 2 to give a k_{ass} of 3×10^3 M^{-1} s^{-1} for SCCA2 (solid line) and 1.65×10^5 M^{-1} s^{-1} for the mutant (dashed line).

RSL somewhere near the conventional P1−P1′, then a C-terminal cleavage product with a molecular mass of ~4 kDa should be detected. For the SCCA2−papain mixture, a single fragment was detected (M_r = 4433.09), placing the cleavage site between the ValP2 and the GluP1 (Figure 5). For the SCCA2−catS interaction, two prominent peaks were detected (M_r = 4432.97 and 4632.23). This placed one

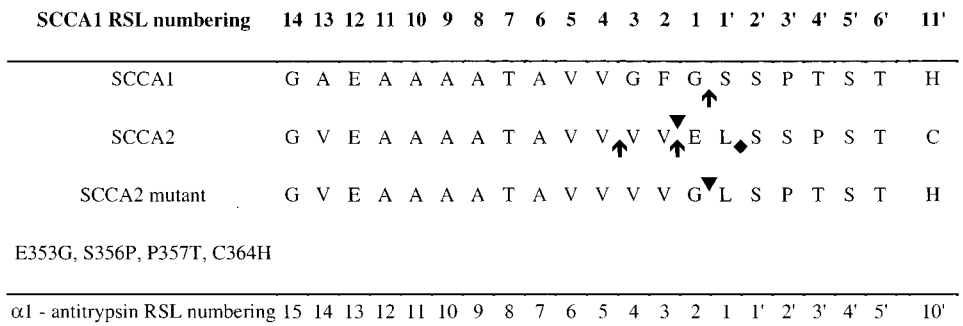

FIGURE 5: Alignment of SCCA1, SCCA2, and the SCCA2 mutant [E353G, S356P, P357T, C364H] RSLs. Numbering on the top line refers to the numbering used for SCCA1 (Table 1). Cleavage positions of catS (↑), papain (▼), and catG (◆) within the RSL are shown as determined from the MALDI MS data and from amino terminal sequencing published previously (*4*, *5*). Numbering on the bottom line refers to the Schechter−Berger numbering scheme (*26*) for α1-antitrypsin.

cleavage at the same position noted for papain and a second site between ValP4 and ValP3 (Figure 5). The presence of two cleavage sites probably reflects the preference of a Val residue at the S2 subsite of catS (*14*, *31*). In contrast to wild-type SCCA2, when the mutant SCCA2 [Glu353Gly, Ser356Pro, Pro357Thr, Cys364His] was mixed with papain, a different peak was detected (M_r = 4375.72). These data suggested that these mutations facilitated the cleavage at the P1−P1′ (Gly-Leu) bond (Figure 5). Although shifting the cleavage site C-terminal 1 residue would still place a Val residue (P2 instead of P3) into the critical S2 subsite of the protease, the relative increase in RSL length might account for the increase in the inhibitory rate constant.

Modeling. To better understand the effect of the ProP3′ on proteinase−inhibitor interaction, we made models of catL, K, and S docked to a theoretical model of SCCA1. The model of SCCA1 was generated by approximation to the solved crystal structure of α1-antitrypsin. Figure 6 shows the model of the docking complex between catL and SCCA1. No attempt was made to model the loop between the C- and the D-helices in SCCA1 as this region contains a 13-residue insertion with respect to α1-antitrypsin. Both the GlyP1 and the GlyP3 residues are in allowed "+ +" conformations. The PheP2 residue is buried in the hydrophobic S2 subsite, and we predict that ProP3′ makes a tight turn out of the active site and stacks against Trp276. There is considerable homology between catL, K, and S (55−58%), and the interactions described above were observed also for the catK−SCCA1 and the catS (theoretical model)−SCCA1 (not shown) docking models.

DISCUSSION

The purpose of this study was to determine why the nearly identical serpins SCCA1 and SCCA2 demonstrated a 50-fold difference in their abilities to inhibit the papain-like cysteine proteinase, catS. Since the RSL of SCCA1 is responsible for cysteine proteinase inhibitory activity, and the RSLs differ by only eight residues, we hypothesized that some (or all) of these nonconservative differences accounted for the discrepancy in inhibitory activity. Using site-directed mutagenesis, we constructed SCCA1 and SCCA2 molecules containing one or more mutations in their RSLs and analyzed kinetically their ability to inhibit catS. The mutations revealed a range of effects and showed that no single residue could convert SCCA2 into a potent cysteine proteinase inhibitor. Rather, certain mutations led to incremental increases in catS inhibitory activity with changes in four positions (P1, P3′, P4′, and P11′) accounting for 80% of the difference in activity between SCCA1 and SCCA2. Moreover, these data established the importance of a Pro residue in the P3′ position for efficient inhibition of catS by both wild-type SCCA1 and mutated SCCA2.

In general, the differences in the RSLs between SCCA1 and SCCA2 can be grouped into two regions, the hinges and the reactive center. The proximal and distal hinge regions affect RSL availability and mobility (*32*). The hinge regions contribute to overall inhibitory activity by participating in the serpin conformational changes that trap the bound proteinase. The hinge regions are unlikely to affect proteinase binding directly but could have an effect if mutations alter the availability of the reactive center. In the proximal hinge region, SCCA1 and SCCA2 differed at the P13 position. Previous studies showed that if Thr was substituted for Ala, SCCA1 showed a 4-fold increase in the second-order rate constant for catS inhibition (*13*). However, substitution of this residue into the proximal hinge region of SCCA2 had little effect on overall catS inhibitory activity by itself or in combination with other RSL mutations. Most likely, the beneficial effects of this residue are best appreciated in the context of the wild-type SCCA1 RSL or possibly the SCCA1 backbone. The variant P11′ position in the distal hinge region proved to be more revealing. Replacing the His residue in SCCA1 with the Cys residue in SCCA2 diminished SCCA1 inhibitory activity about 20%. Conversely, substitution of the Cys residue in SCCA2 with the His residue in SCCA1 had by itself only a marginal effect on the ability of SCCA2 to inhibit catS. However, the effects of the His residue became apparent in a mutant SCCA2 molecule that also contained SCCA1 residues at the P1, P3′, and P4′ positions. Thus, the His residue in the P11′ position contributed to catS inhibitory activity providing that important residues (e.g., P1−P4′) in the RSL binding site were present.

The reactive center contributes to overall inhibitory activity by functioning as a pseudo-substrate. Thus, residues in this portion of the RSL are related intimately to the active site of the proteinase and will effect binding, cleavage, and covalent bond formation. For papain-like cysteine proteinases, the P2 rather than the P1 residue is one of the most important determinants of specificity and binding. In the case of catS and papain, the preferred P2 residues are bulky hydrophobics (*14*, *15*). The P2 residue in SCCA1 and SCCA2 are Phe and Val, respectively. Mutation of this

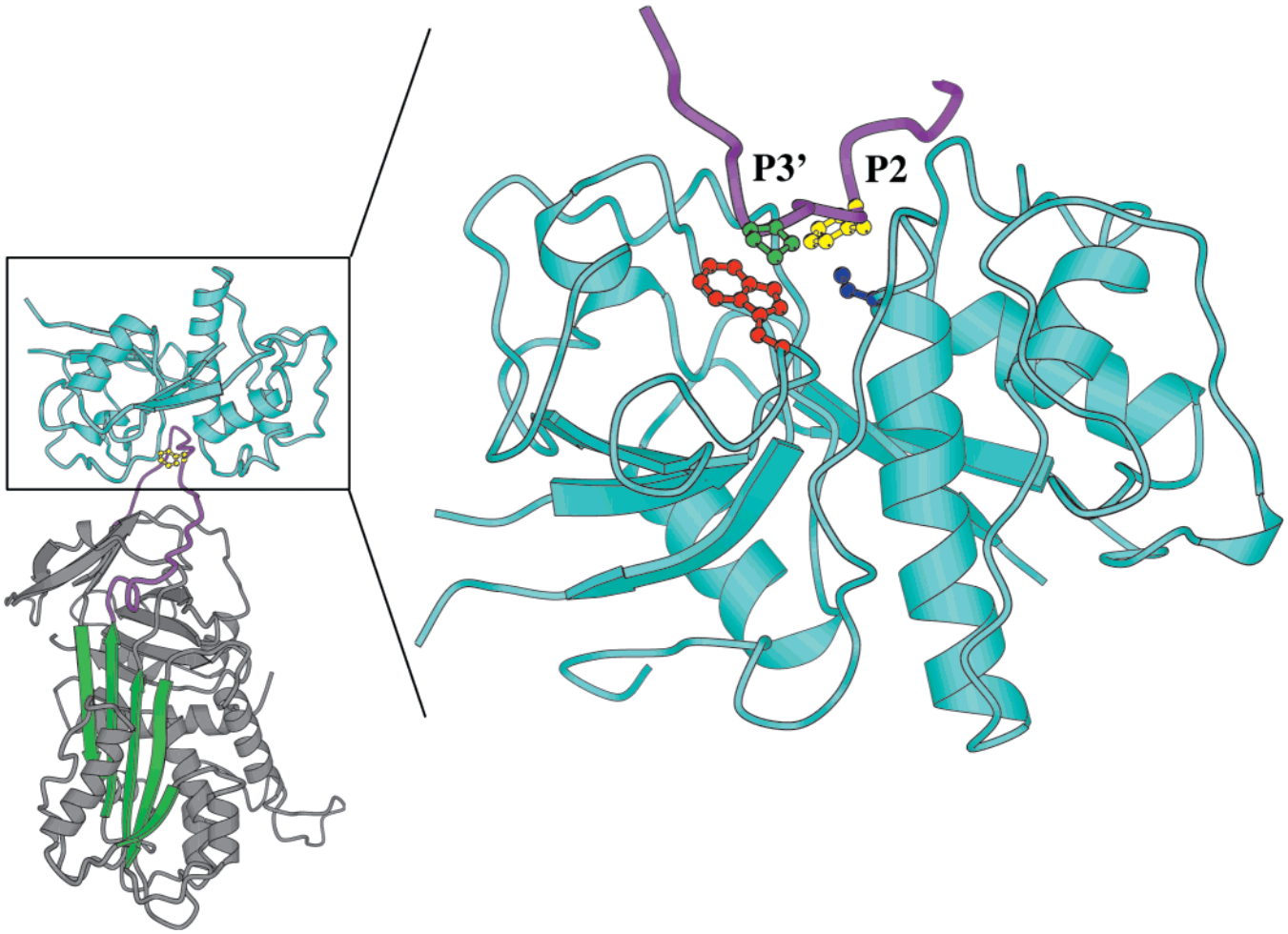

FIGURE 6: Molecular modeling of cathepsin−SCCA1 interaction. (Left) Model of the docking complex between catL and SCCA1. The RSL of the serpin is in magenta, the A-sheet is in green, and the rest of the molecule is in gray. CatL is shown in cyan. The figure was prepared using Molscript (*42*). (Right) The active site cleft of catL with the RSL of SCCA1 in purple. The catalytic cysteine of catL is shown in dark blue ball-and-stick, and the conserved Trp276 is in red. The ProP3′ (in green ball-and-stick) stacks against Trp276 and makes a tight turn out of the active site of the protease. The P2 residue of SCCA1 is shown in yellow ball-and-stick. To expose the RSL−active site interaction, the figure is rotated 180° horizontally with respect to its position within the left-side panel.

residue to a nonconsensus residue, such as Ala, abolished the ability of SCCA1 to inhibit catS (*13*). Interestingly, neither catS nor papain utilizes the ValP2 of SCCA2 at the S2 subsite. Rather, the RSL cleavage data show that the ValP6 (catS) or the ValP4 (catS and papain) actually serve as the functional P2 residues (Figure 5). This observation may explain why conversion of the SCCA2 P2 residue to Phe was in itself unable to increase appreciably catS inhibitory activity. Thus, these findings suggested that so long as the actual P2 residue was one of those preferred by catS, other RSL mutations were required to make SCCA2 a more potent inhibitor of catS. Subsequent mutations confirmed this notion and showed that the P1, P3′ (possibly the P4′), and P11′ residues were the most important.

For the SCCA1−catS interaction, the GlyP1 could be mutated to a Glu residue (wild-type for SCCA2) without any ill effects. However, replacement with an Arg residue decreased catS inhibitory activity by 80% (*13*). This finding suggested that charge, rather than the size of the side-chain, may be an important factor in binding and subsequent peptide bond hydrolysis. In contrast to SCCA1, the SCCA2 P1 mutant [Glu353Gly] showed that the GlyP1 was important for catS inhibition. If we assume that the wild-type RSL of SCCA2 (unlike that of SCCA1) is less than a perfect fit for the catS binding site, then a Gly residue in the P1 position could contribute to the inhibitory activity by increasing rotational flexibility of the RSL. In turn, this increased flexibility might decrease steric clashes or electrostatic effects and (as suggested by the RSL cleavage data) allow for the ValP2 to fit into the S2 subsite. Indeed, either compensatory or interdependent interactions between peptide subsites of the proteinase or an order of residue interaction can contribute to the binding and inhibition reaction (*33*).

Perhaps the most surprising aspect of this study was the requirement for Pro and Thr residues at the P3′ and P4′ positions, respectively. Although peptide cleavage studies suggested that Pro rather than Thr was the critical residue, we did not perform mutational studies that evaluated their contributions independently. To our knowledge, the P3′ residue was not considered to be an important determinant of catS inhibition. Nonetheless, changes to the P3′ residue strongly modulated the catS inhibitory activity of these serpins. Replacement of the ProP3′ with a Gly residue decreased by ~90% the rate of catS inhibition by SCCA1. Conversely, shifting the ProP4′ of the SCCA2 RSL to the P3′ position resulted in a 5-fold increase in the rate of catS inhibition. However, there was a more dramatic increase in inhibitory activity when the mutations were combined with

mutations at the P1 [Glu353Gly] and P11′ [Cys363His] positions. Most likely, the [Ser353Pro, Pro354Thr] mutations also facilitated a change (at least for papain) of the cleavage site from between the P3−P2 residues to between the P2 and the P1 residues. Thus, a Pro in the P3′ position might facilitate a better fit of the RSL into the active site of the proteinase. It is well-known that, within limits, serpins are capable of utilizing different residues in their RSL to inhibit different types of proteinases (*34*−*37*). For example, proteinase inhibitor 8 is cleaved by thrombin between Arg339 and Cys340 (P1−P1′), while chymotrypsin cleaves between Ser341 and Arg342 (P2′−P3′) (*35*). However, it is not known how far upstream or downstream of the canonical (α1-antitrypsin numbering) P1-residue that cleavage can occur and still have the serpin serve as an inhibitor rather than a simple substrate. The detection of a cleavage after the archetypal P5 and P3 residues in the SCCA2−catS interaction along with a low SI (1.3) suggested that RSL cleavage this far N-terminal may still allow for effective inhibition.

The presence of a S3′ site in the papain-like cysteine proteinases has not been fully explored. To date, most analysis of substrate specificity of cysteine or serine proteinases concentrated on the residues just upstream (P3−P1) or downstream (P1′ and P2′) of the cleavage site (*31*, *33*, *38*, *39*). Furthermore, molecular modeling of the papain-like cysteine proteinases with and without inhibitors suggested that there was no S3′ subsite (*29*), but the cleavage of small peptides by the papain-like cysteine proteinase, cruzain, is facilitated by the addition of a P3′Pro to the substrate (*30*).

Can the effect of the P3′Pro in the interactions of substrates with cruzain and catS be accounted for in the absence of a S3′ subsite? The reactive site clefts of the papain-like cysteine proteinases are short. If the P3′Pro were to place a kink in the peptide or RSL and rest on the outside edge of the binding cleft, then this residue might serve to align the P2 and other residues with the corresponding enzyme subsites. Indeed, modeling of the catL−SCCA1 complex revealed that the ProP3′ made a tight turn out of the active site of the proteinase and that this residue stacked against the side chain of Trp276 in catL. Trp276 is two residues C-terminal to the catalytic Asn and forms part of the highly conserved "NSW" motif in papain-like cysteine proteinases. An identical interaction was observed in the models of the catK−SCCA1 and catS−SCCA1 complexes. Interestingly, Thompson et al. (*24*) note that the Z-group of the benzoyl-Tyr-Ala-fluoromethyl ketone inhibitor makes a similar hydrophobic staking interaction with the corresponding Trp residue in catK. We suggest that much of the reduction in the rate of catS inhibition by the SCCA1 P3′ mutant [Pro356Gly] was due to the inability of the Gly at the P3′ position to interact properly with the conserved Trp residue. In addition, the increased flexibility around this Gly residue may have relaxed the RSL to the extent that it was unable to make a rigid turn out of the active site, thereby affecting the rate of binding or peptide bond hydrolysis.

The effect of a kink in the substrate may be relevant to other proteinases but is clearly dependent on the shape and curvature of the substrate binding cleft in the proteinase. For example, unlike the papain-like cysteine proteinase, the common serine proteinases, such as trypsin and chymotrypsin, have long reactive site clefts that extend beyond both P5 and P5′ (*40*). Indeed, the serine proteinase from the fiddler crab, serine collagenase 1, which is similar to chymotrypsin, has an extended binding cleft making specific contacts with the substrate from P7−P4′ (*41*). Proteinases with long reactive site clefts may be sensitive to the strong influence that a Pro residue can have on the peptide conformation, thereby affecting the affinity of the proteinase for the peptide. Thus, it is conceivable that serpins have evolved to inhibit active sites of different sizes by selecting for certain residues in the P′ region to ensure that the reactive center of the RSL is in register with catalytic machinery of the enzyme.

ACKNOWLEDGMENT

We thank Amy Elias for preparing the manuscript.

REFERENCES

1. Hunt, L. T., and Dayhoff, M. O. (1980) *Biochem. Biophys. Res. Commun. 95*, 864−871.
2. Gettins, P. G. W., Patston, P. A., and Olson, S. T. (1996) in *Molecular Biology Intelligence Unit*, p 202, R. G. Landes Company and Chapman & Hall, Austin, TX.
3. Schneider, S. S., Schick, C., Fish, K. E., Miller, E., Pena, J. C., Treter, S. D., Hui, S. M., and Silverman, G. A. (1995) *Proc. Natl. Acad. Sci. U.S.A. 92*, 3147−3151.
4. Schick, C., Pemberton, P. A., Shi, G.-P., Kamachi, Y., Cataltepe, S., Bartuski, A. J., Gornstein, E. R., Bromme, D., Chapman, H. A., and Silverman, G. A. (1998) *Biochemistry 37*, 5258−5266.
5. Schick, C., Kamachi, Y., Bartuski, A. J., Cataltepe, S., Schechter, N. M., Pemberton, P. A., and Silverman, G. A. (1997) *J. Biol. Chem. 272*, 1849−1855.
6. Travis, J., Guzdek, A., Potempa, J., and Watorek, W. (1990) *Biol. Chem. Hoppe-Seyler 71*, 3−11.
7. Patston, P. A., Gettins, P., Beechem, J., and Schapira, M. (1991) *Biochemistry 30*, 8876−8882.
8. Carrell, R. W., and Evans, D. L. I. (1992) *Curr. Opin. Struct. Biol. 2*, 438−446.
9. Stratikos, E., and Gettins, P. G. (1999) *Proc. Natl. Acad. Sci. U.S.A. 96*, 4808−4813.
10. Plotnick, M. I., Mayne, L., Schechter, N. M., and Rubin, H. (1996) *Biochemistry 35*, 7586−7590.
11. Matheson, N. R., van Halbeek, H., and Travis, J. (1991) *J. Biol. Chem. 266*, 13489−13491.
12. Huntington, J. A., Fan, B., Karlsson, K. E., Deinum, J., Lawrence, D. A., and Gettins, P. G. W. (1997) *Biochemistry 36*, 5432−5440.
13. Schick, C., Bromme, D., Bartuski, A. J., Uemura, Y., Schechter, N. M., and Silverman, G. A. (1998) *Proc. Natl. Acad. Sci. U.S.A. 95*, 13465−13470.
14. Brömme, D., Bonneau, P. R., Lachance, P., and Storer, A. C. (1994) *J. Biol. Chem. 269*, 30238−30242.
15. Brömme, D., Bonneau, P. R., Lachance, P., Wiederanders, B., Kirschke, H., Peters, C., Thomas, D. Y., Storer, A. C., and Vernet, T. (1993) *J. Biol. Chem. 268*, 4832−4838.
16. Banda, M. J., Werb, Z., and McKerrow, J. H. (1987) *Methods Enzymol. 144*, 288−305.
17. Shi, G.-P., Munger, J. S., Meara, J. P., Rich, D. H., and Chapman, H. A. (1992) *J. Biol. Chem. 267*, 7258−7262.
18. Morrison, J. F., and Walsh, C. T. (1988) *Adv. Enzymol. Relat. Areas Mol. Biol. 61*, 201−301.
19. Beatty, K., Bieth, J., and Travis, J. (1980) *J. Biol. Chem. 255*, 3931−3934.
20. Hirata, Y., Cezari, M. H. S., Nakaie, C. R., Boschcov, P., Ito, A. S., Juliano, A. M., and Juliano, L. (1994) *Lett. Pept. Sci. 1*, 299−308.
21. Csuhai, E., Juliano, M. A., Pyrek, J., Harms, A., Juliano, L., and Hersh, L. B. (1999) *Anal. Biochem. 269*, 149−154.
22. Sali, A., and Blundell, T. L. (1993) *J. Mol. Biol. 234*, 779−815.

23. Coulombe, R., Grochulski, P., Sivaraman, J., Menard, R., Mort, J. S., and Cygler, M. (1996) *EMBO J. 15*, 5492−5503.
24. Thompson, S. K., Halbert, S. M., Bossard, M. J., Tomaszek, T. A., Levy, M. A., Zhao, B., Smith, W. W., Abdel-Meguid, S. S., Janson, C. A., D'Alessio, K. J., McQueney, M. S., Amegadzie, B. Y., Hanning, C. R., DesJarlais, R. L., Briand, J., Sarkar, S. K., Huddleston, M. J., Ijames, C. F., Carr, S. A., Garnes, K. T., Shu, A., Heys, J. R., Bradbeer, J., Zembryki, D., Veber, D. F., et al. (1997) *Proc. Natl. Acad. Sci. U.S.A. 94*, 14249−14254.
25. Fengler, A., and Brandt, W. (1998) *Protein Eng. 11*, 1007−1113.
26. Schechter, I., and Berger, A. (1967) *Biochem. Biophys. Res. Commun. 27*, 157−162.
27. Huber, R., and Carrell, R. W. (1989) *Biochemistry 28*, 8951−8966.
28. Lawrence, D. A., Olson, S. T., Palaniappan, S., and Ginsburg, D. (1994) *J. Biol. Chem. 269*, 27657−27662.
29. Turk, D., Guncar, G., Podobnik, M., and Turk, B. (1998) *Biol. Chem. 379*, 137−147.
30. Nery, E. D., Juliano, M. A., Meldal, M., Svendsen, I., Scharfstein, J., Walmsley, A., and Juliano, L. (1997) *Biochem. J. 323*, 427−433.
31. Brömme, D., and Kirschke, H. (1993) *FEBS Lett. 322*, 211−304.
32. Stein, P. E., and Carrell, R. W. (1995) *Nat. Struct. Biol. 2*, 96−113.
33. Schellenberger, V., Turck, C. W., and Rutter, W. J. (1994) *Biochemistry 33*, 4251−7.
34. Dahl, S. W., Rasmussen, S. K., and Hejgaard, J. (1996) *J. Biol. Chem. 271*, 25083−25088.
35. Dahlen, J. R., Foster, D. C., and Kisiel, W. (1998) *Biochem. Biophys. Res. Commun. 244*, 172−177.
36. Aulak, K. S., Davis, A. E., III, Donaldson, V. H., and Harrison, R. A. (1993) *Protein Sci. 2*, 727−732.
37. Potempa, J., Shieh, B.-H., and Travis, J. (1988) *Science 241*, 699−700.
38. Schuster, M., Kasche, V., and Jakubke, H. D. (1992) *Biochim. Biophys. Acta 1121*, 207−12.
39. Menard, R., Carmona, E., Plouffe, C., Brömme, D., Konishi, Y., Lefebvre, J., and Storer, A. C. (1993) *FEBS Lett. 328*, 107−110.
40. Perona, J. J., and Craik, C. S. (1995) *Protein Sci. 4*, 337−360.
41. Perona, J. J., Tsu, C. A., Craik, C. S., and Fletterick, R. J. (1997) *Biochemistry 36*, 5381−5392.
42. Kraulis, P. J. (1991) *J. Appl. Crystallogr. 24*, 946−950.

BI000050G